URSI GASS 2020, Rome, Italy, 29 August - 5 September 2020

Teaching radiofrequency power measurements

Carlo F. M. Carobbi
Department of Information Engineering, University of Florence, Firenze, Italy

Abstract

A method is here proposed to teach radiofrequency (RF) power measurements to master's degree students in electronics and communications engineering. Before going into the details of the principle of operation and architecture of power meters (not discussed here) the topic of power measurement is introduced emphasizing the fact that power generators and meters are calibrated to indicate the power delivered to, or absorbed by, a perfect Z_0 (e.g. 50 Ω) load. Then, it is discussed what happens when this perfect Z_0 load assumption is not satisfied introducing the mismatch correction. The mismatch correction is analyzed in terms of uncertainty governed by the U-shaped probability density function (PDF). The U-shaped PDF gives the opportunity to discuss state-of-knowledge PDFs whose use is ubiquitous in measurement uncertainty estimation. Indeed, such U-shaped PDF is not the result of direct observation of the physical world, it reflects the state of knowledge of the experimenter about the physical phenomenon. These concepts are finally applied to a simple estimation of RF power measurement uncertainty, showing that mismatch is, as frequently occurs in precision power measurements, the dominant contribution to uncertainty.

1 Introduction

Power measurements are among the most accurate in RF measurement technique. A power meter (for absolute scalar measurement) and a vector network analyzer (for relative vector measurement) are the building blocks of the measurement traceability of an RF laboratory. The scope here is to illustrate how metrological concepts related to RF power measurement can be introduced to master's degree students in electronics and communications engineering. Stimulating the interest of students in assessing the quality of measurement results is of paramount importance due to the rapid growth, in the last twenty years, of the investment in improving testing and calibration. Key factors promoting this process are, together with advancements in RF technology, the publication of the Guide to the expression of Uncertainty in Measurement (briefly the GUM, [1]) and the increasing number of testing and calibration laboratories accredited to ISO/IEC 17025 [2]. This is witnessed by several recent papers of the same author devoted to the quality of testing and calibration in the specific sector of electromagnetic compatibility [3-20].

2 Power transfer between a source and a load

Students must have a solid background knowledge of electromagnetic wave propagation in transmission lines and of scattering parameters. This is the main reason why the concepts introduced in this paper are provided to master's degree students. Indeed, propagation and network parameters are usually the subject of applied electromagnetics and network theory teachings provided during the bachelor's degree in electronics and communications engineering. I preliminarily recall that scattering parameters always exist, while the impedance or admittance parameters, for example, do not. This depends on the structure of the network (and I make simple examples). Further, for reciprocal networks $S_{ij} = S_{ji}$ if $i \neq j$, for lossless networks $\overline{\overline{S}}\left[\left(\overline{\overline{S}}\right)^*\right]^T = I$ (where $\overline{\overline{S}}$ is the matrix of the scattering parameters, T indicates "transposed", * indicates "conjugate" and I is the identity matrix) and for a two-port symmetric network $S_{11} = S_{22}$.

I introduce the power transfer between a source and a load through a sketch like the one represented in Figure 1, where a source is connected to a load through a connection, which may be a cable, an adapter, an attenuator, an amplifier or a combination thereof. The source can represent the output of an RF generator or of a power amplifier, a receiving antenna, or another power delivering device. Similarly, the load can represent the input of a spectrum analyzer or a power meter, a transmitting antenna, or another power absorbing device.

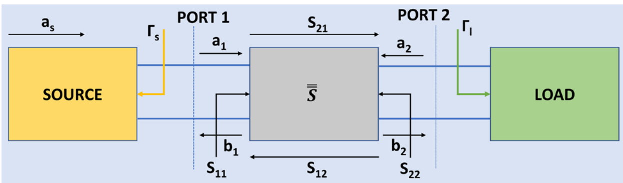

Figure 1. Sketch of the connection between a source and a load through a two-port network represented by its scattering matrix $\overline{\overline{S}}$.

Let Γ_S and Γ_L represent the output reflection coefficients of the source and of the load, respectively. Symbols a_i and b_i, $i = 1,2$, represent incident and reflected waves, respectively. The measurement unit of the squared magnitude of incident and reflected waves is watt (symbol W). $|a_i|^2$ represents the incident power, while $|b_i|^2$ represents the reflected power. The reflection coefficients as well as the parameters of the scattering matrix are referred to a real Z_0 impedance. In practice two options are possible for Z_0, namely $Z_0 = 50$ Ω or $Z_0 = 75$ Ω. In metrological applications $Z_0 = 50\ \Omega$, while in video applications (e.g. broadcast TV receivers and antennas) $Z_0 = 75\ \Omega$.

Through the analysis of the network represented in Figure 1 the following set of equations is easily derived

$$\begin{cases} a_1 = a_S + b_1\Gamma_S \\ a_2 = \Gamma_L b_2 \\ b_1 = S_{11}a_1 + S_{12}a_2 \\ b_2 = S_{21}a_1 + S_{22}a_2 \end{cases}. \tag{1}$$

Note that a_S represents the wave that the source would deliver to a load whose impedance is Z_0 ($b_1 = 0$, the "matched load"), or the wave that a source having internal impedance Z_0 ($\Gamma_S = 0$) would deliver to any load.

By solving the system of equations (1) (tedious but straightforward) we obtain the incident wave to the load

$$b_2 = \frac{S_{21}a_S}{(1-\Gamma_S S_{11})(1-\Gamma_L S_{22}) - \Gamma_S\Gamma_L S_{12}S_{21}}, \tag{2}$$

from which the incident power, the reflected power and the absorbed power are immediately obtained as $|b_2|^2$, $|b_2\Gamma_L|^2$ and $|b_2|^2\left(1-|\Gamma_L|^2\right)$, respectively.

3 Direct connection

It is worth simplifying (2) in the case of a direct connection between the source and the load. This means that $S_{11} = S_{22} = 0$ and $S_{12} = S_{21} = 1$, hence from (2)

$$b_2 = \frac{a_S}{1-\Gamma_S\Gamma_L} \tag{3}$$

(3) is simple but suggests several considerations. It is important to distinguish between the "matched load" and the "conjugate matched load". In the case of a matched load $\Gamma_L = 0$. The reflected power is zero and the power absorbed is

$$P_0 = |a_S|^2. \tag{4}$$

For a conjugate matched load $\Gamma_L = \Gamma_S^*$. The peculiarity of the conjugate matched load is that it absorbs all the available power from the source, which is

$$P_S = \frac{|a_S|^2}{1-|\Gamma_S|^2}. \tag{5}$$

If, and only if, $\Gamma_S = 0$ then $P_S = P_0$. Conjugate match is rarely implemented in a RF measurement setup. Conversely:

- *RF power generators* are calibrated to indicate the power delivered to the matched load P_0 ,
- *RF power meters* are calibrated to indicate the power that would be absorbed by the matched load P_0.

This is quite important to know in order to correctly interpret the operation and specifications of power sources and power meters.

In RF literature the term $(1-\Gamma_L\Gamma_S)^{-1}$ is often referred to as "correction for multiple reflections." The curious student might ask why. This originates from assuming that waves are bouncing between the source and the load due to mismatch at both sides. A time domain reasoning is followed even if (3) applies to the sinusoidal regime. The first (as time increases) wave a_0 leaving the generator and travelling toward the load does not "realize" that the load is mismatched until it reaches it. Hence $w_0 = a_S$ is the first wave travelling from the source to the load. This first wave is in part reflected and in part absorbed by the load. The reflected portion $\Gamma_L a_0$ is then in part absorbed and in part reflected by the source, thus generating a second wave $w_1 = \Gamma_S\Gamma_L w_0$ that propagates toward the load. This second wave undergoes the same process as the first wave thus producing a third wave that propagates toward the load, namely $w_2 = \Gamma_S\Gamma_L w_1$. The superposition of these waves propagating toward the load is b_2 . In mathematical terms

$$b_2 = \sum_{k=0}^{\infty} w_k = a_S \sum_{k=0}^{\infty} (\Gamma_S\Gamma_L)^k \tag{6}$$

It is immediate to derive (3) from (6) since $\sum_{k=0}^{\infty} (\Gamma_S\Gamma_L)^k = \frac{1}{1-\Gamma_S\Gamma_L}$.

4 Power measurement

The power absorbed by a power meter from a source is obtained from (3) and given by

$$P_L = \frac{P_0\left(1-|\Gamma_L|^2\right)}{|1-\Gamma_S\Gamma_L|^2}. \tag{7}$$

This power P_L is not entirely absorbed by the sensing element of the power meter (e.g. a thermistor). A small portion of P_L is lost in radiation, metallic and dielectric losses. The fraction absorbed by the sensing element is the one sensed, and it is given by

$$P_M = \eta P_L = \frac{\eta P_0\left(1-|\Gamma_L|^2\right)}{|1-\Gamma_S\Gamma_L|^2}, \tag{8}$$

where η is the efficiency of the power meter. Since the power meter is calibrated to indicate P_0 then the measured power P_M shall be corrected as follows

$$P_0 = \frac{|1-\Gamma_S\Gamma_L|^2}{\eta\left(1-|\Gamma_L|^2\right)} P_M. \tag{9}$$

We now define $c_F = \eta\left(1-|\Gamma_L|^2\right)$ as the calibration factor of the power meter and

$$m = |1-\Gamma_S\Gamma_L|^2 \tag{10}$$

as the mismatch correction. Hence, from (9) we have

$$P_0 = \frac{m}{c_F} P_M. \tag{11}$$

The calibration factor of the power meter is provided by the manufacturer or obtained from a calibration certificate, in terms of an estimate and uncertainty. The mismatch correction depends on the output reflection coefficient of the source; thus, it depends on the specific source under measurement. This means that the mismatch correction cannot be evaluated through the calibration of the power meter. The mismatch correction could, in principle, be applied in the calibration of the power meter, for the specific source used in the calibration setup, in order to reduce the uncertainty of the calibration factor.

5 Mismatch uncertainty

It is now important to observe that the mismatch correction depends on both the magnitude and phase of the product $\Gamma_S\Gamma_L$. Such rich information is generally unavailable, even for the specific source and power meter used. Therefore, the mismatch correction cannot be applied. The maximum warranted magnitude of Γ_S and Γ_L can however be deduced from specifications, calibrations, or other sources of information about the performance of the source and power meter. What is therefore available is not the specific correction value but its maximum and minimum values

$$m_- = \left(1-\left|\Gamma_S\Gamma_L\right|\right)^2$$
$$m_+ = \left(1+\left|\Gamma_S\Gamma_L\right|\right)^2 . \quad (12)$$

Knowledge of m_- and m_+ permits to deal with mismatch correction through a worst case, deterministic analysis. Modern evaluation of uncertainty is based however on a probabilistic (rather than deterministic) analysis leading to a narrower value of the range of the possible values of the measurand. A probability of including the true value of the measurand is also associated to such range which is particularly significant when the measurement result is the basis for an assessment of compliance against a tolerance. Tolerance is indeed met or not met with a certain probability and this information is useful, for example, to estimate the number of conforming or non-conforming samples in a production lot.

If the mismatch correction is not applied, then mismatch causes a measurement error whose limits are known from (12). How can we deal with mismatch error through a probabilistic approach? The answer is as follows.

Let us consider (10). After a simple mathematical derivation, we obtain

$$m = 1-2\left|\Gamma_S\Gamma_L\right|\cos\varphi+\left|\Gamma_S\Gamma_L\right|^2, \quad (13)$$

where $\varphi = \arg\left(\Gamma_S\Gamma_L\right)$. φ is unknown but surely comprised between 0 and π or between $-\pi$ and 0. φ is now interpreted as a random variable and since no information is available about its probability distribution then a uniform PDF is assigned to it (ignorance is uniform!).

It is easy to show that if φ is a uniformly distributed random variable in $[0,\pi]$ then $\cos\varphi$ is a random variable having a symmetric U-shaped PDF with expected value 0 and standard deviation $1/\sqrt{2}$. Figure 2 provides a representation of the transformation from uniform to U-shaped PDF through uniform sampling of the period *P* of a sinusoid.

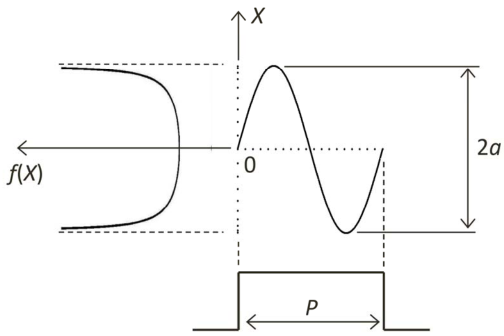

Figure 2. Transformation from uniform to U-shaped PDF.

The U-shaped PDF shown in Figure 2 is

$$f\left(X\right) = \frac{1}{\pi\sqrt{a^2-X^2}}, \left|X\right| < a \quad (14)$$

and $f\left(X\right)=0$ if $\left|X\right| > a$.

Mismatch uncertainty is frequently dealt with in log- instead of linear units. Then the mismatch correction is

$$M = 10\log_{10} m \quad (15)$$

It is shown in [6] that the expected value of *M* is zero and the standard uncertainty is approximately $\frac{8,686}{\sqrt{2}}\left|\Gamma_S\Gamma_L\right|$.

6 Example

Suppose that the reading of a power meter when connected to a power source is −20,37 dBm. The calibration factor of the power meter, as provided by its certificate of calibration, is −0,23 dB with an expanded uncertainty of 0,26 dB (coverage factor $k = 2$, corresponding to a coverage probability of 95 % assuming a normal PDF). From specifications of both the power source and power meter we deduce $\left|\Gamma_S\right| = 1/3$ and $\left|\Gamma_S\right| = 1/5$, hence the standard uncertainty is 0,41 dB. The estimate of the source power is therefore −20,37 dBm + 0,23 dB = −20,14 dBm and the combined standard uncertainty is

$$u(p) = \sqrt{\left(0.26/2\right)^2+\left(0.41\right)^2} \text{ dB} = 0.43 \text{ dB} \quad (16)$$

In order to evaluate the expanded uncertainty, it is to be acknowledged that the non-normal (U-shaped) mismatch contribution dominates over the normal contribution associated with the calibration factor. Therefore, the central limit theorem is not applicable. From a Monte Carlo uncertainty analysis, it is found that the PDF is quite different from the normal one (red dashed line in Figure 3) and much more like a U-shaped PDF (bleu continuous line in Figure 3). The coverage factor corresponding to the stipulated 95 % coverage probability is 1,6 and the expanded uncertainty is 0,70 dB. The plot in Figure 2 was obtained by using NIST Uncertainty Machine, a free internet resource made available by NIST for Monte Carlo uncertainty analysis.

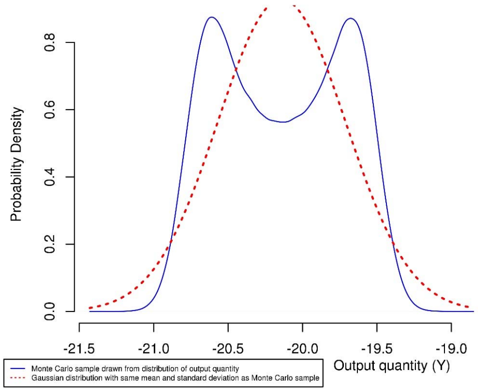

Figure 3. PDF of the measured power as obtained through NIST Uncertainty Machine.

7 References

1. BIPM, IEC, IFCC, ILAC, ISO, IUPAC, IUPAP and OIML, 2008 Guide to the Expression of Uncertainty in Measurement, JCGM 100:2008, GUM 1995 with minor corrections.

2. General requirements for the competence of testing and calibration laboratories, ISO/IEC 17025:2005.

3. C. F. M. Carobbi, M. Cati, C. Panconi, "Reproducibility of Radiated Emissions Measurements in Compact, Fully–Anechoic, Rooms — The Contribution of the Site-to-Site Variations," IEEE Trans. on EMC, vol. 51, no. 3, pp. 574-582, Aug. 2009.

4. C. F. M. Carobbi and L. M. Millanta, "Circuit Loading in Radio-Frequency Current Measurements: The Insertion Impedance of the Transformer Probes," IEEE Trans. on I&M, vol. 59, no. 1, pp. 200-204, Jan. 2010.

5. C. F. M. Carobbi, M. Cati, C. Panconi, "A Double Inequality for Equivalent Impulse Bandwidth," IEEE Trans. on EMC, vol. 52, no. 3, pp. 516-520, Aug. 2010.

6. C. F. M. Carobbi, M. Cati, C. Panconi, "Note on the Expected Value and Standard Deviation of the Mismatch Correction," IEEE Trans. on EMC, vol. 53, no. 4, pp. 1098-1099, Nov. 2011.

7. C. F. M. Carobbi and M. Stecher, "The Effect of the Imperfect Realization of the Artificial Mains Network Impedance on the Reproducibility of Conducted Emission Measurements," IEEE Trans. on EMC, vol. 54, no. 5, pp. 986-997, Oct. 2012.

8. C. F. M. Carobbi, A. Bonci, M. Stellini and M. Borsero, "Time-Domain Characterization of the Surge, EFT/Burst and ESD Measurement Systems," IEEE Trans. on Instrumentation and Measurement, vol. 62, no. 6, pp. 1840-1846, Jun. 2013.

9. C. F. M. Carobbi, "Measurement Error of the Standard Unidirectional Impulse Waveforms Due to the Limited Bandwidth of the Measuring System," IEEE Trans. on EMC, vol. 55, no. 4, pp. 692-698, Aug. 2013.

10. C. F. M. Carobbi and A. Bonci, "Elementary and Ideal Equivalent Circuit Model of the 1,2/50 – 8/20 μs Combination Wave Generator," IEEE-EMC Magazine, vol. 2, issue 4, pp. 51-57.

11. C. F. M. Carobbi, "Bayesian inference on a squared quantity," Measurement 48 (2014), pp. 13–20.

12. C. F. M. Carobbi, A. Bonci, M. Cati, C. Panconi, M. Borsero and G. Vizio, "Design, Preparation, Conduct and Result of a Proficiency Test of Radiated Emission Measurements", IEEE Trans. on EMC, vol. 56, no. 6, pp. 1251-1261, Dec. 2014.

13. C. Carobbi and F. Pennecchi, "Bayesian conformity assessment in presence of systematic measurement errors," Metrologia 53 (2016) S74–S80.

14. C. F. M. Carobbi, A. Bonci, M. Cati, C. Panconi, M. Borsero and G. Vizio, "Proficiency Testing by Using Traveling Samples With Preassigned Reference Values", IEEE Trans. on EMC, vol. 58, no. 4, pp. 1339 – 1348, Aug. 2016.

15. C. F. M. Carobbi, "Bayesian Inference in Action in EMC – Fundamentals and Applications", IEEE Trans. on EMC, vol. 59, no. 4, pp. 1114 – 1124, Aug. 2017.

16. C. F. M. Carobbi, "The Statistical Field Uniformity Criterion in Transverse Electromagnetic Waveguides," IEEE Trans. on EMC, vol. 59, no. 6, pp. 2052 – 2053, Dec. 2017.

17. C. F. M. Carobbi, and D. Izzo, "Evaluation and Improvement of the Reproducibility of CISPR 25 ALSE Test Method," IEEE Trans. on EMC, vol. 60, no. 4, pp. 1069 – 1077, Aug. 2018.

18. C. F. M. Carobbi, "A Lumped Model of the Rod Antenna Setup Adopted for Military and Automotive Testing," IEEE Trans. on EMC, vol. 61, no. 4, pp. 1289 – 1296, Aug. 2019.

19. C. F. M. Carobbi, S. Lalléchère, and L. R. Arnaut, "Review of Uncertainty Quantification of Measurement and Computational Modeling in EMC Part I: Measurement Uncertainty," IEEE Trans. on EMC, vol. 61, no. 6, pp. 1698 – 1705, Dec. 2019.

20. S. Lalléchère, C. F. M. Carobbi, and L. R. Arnaut, "Review of Uncertainty Quantification of Measurement and Computational Modeling in EMC Part II: Computational Uncertainty," IEEE Trans. on EMC, vol. 61, no. 6, pp. 1699 – 1706, Dec. 2019.